Preprint Title Tailoring the magnetic ordering of the Cr_4O_5/Fe(001) surface via a controlled adsorption of C_{60} organic molecules.

Authors Federico Orlando, Guido Fratesi, Giovanni Onida and Simona Achilli

Publication Date 12 Mär 2020

Article Type Full Research Paper

ORCID® iDs Guido Fratesi - https://orcid.org/0000-0003-1077-7596; Giovanni Onida - https://orcid.org/0000-0001-9532-5083; Simona Achilli - https://orcid.org/0000-0001-6812-5043

Tailoring the magnetic ordering of the Cr_4O_5/Fe(001) surface via a controlled adsorption of C_{60} organic molecules.

Federico Orlando[1], Guido Fratesi[1,2], Giovanni Onida[1,2] and Simona Achilli[*1,2]

Address: [1]Dipartimento di Fisica, Universitá degli Studi di Milano, Via Celoria 16, 20133 Milano and [2]European Theoretical Spectroscopy Facility (ETSF)

Email: Simona Achilli - simona.achilli@unimi.it

[*] Corresponding author

Abstract

We analyse the spinterface formed by a C_{60} molecular layer on a Fe(001) surface covered by a two-dimensional Cr_4O_5 layer. We consider different geometries, by combining the high symmetry adsorption sites of the surface with three possible orientations of the molecules in a fully relaxed Density Functional Theory calculation. We show that the local hybridization between the electronic states of the Cr_4O_5 layer and those of the organic molecules is able to modify the magnetic coupling of the Cr atoms. Both the intra-layer and the inter-layer magnetic interaction is indeed driven by O atoms of the two-dimensional oxide. We demonstrate that the C_{60} adsorption on the energetically most stable site turns the ferromagnetic intra-layer coupling into an antiferromagnetic one, and that antiferromagnetic to ferromagnetic switching and spin patterning of the substrate are made possible by adsorption on other sites.

Keywords

Spinterface, C_{60}, Density Functional Theory, Magnetic patterning,Cr_4O_5

Introduction

The advancements in the field of spintronics are intimately related to the capability to control the magnetic properties of surfaces and interfaces. The magnetic switching of magnetic materials is usually controlled via externally applied magnetic field or by electric-field driven means [1], as spin torque methods, that requires large currents and complex setup and guarantee low efficiency in the process [2]. On the other hand, magnetic behavior at surfaces can be induced or modified through the adsorption of foreign species and molecules and by the growth of magnetic thin films [3-7]. In past years it has been established that spin selective electron transfer through chiral molecules is able to magnetize the underlying substrate and induce a magnetic switching [8].

In recent times, organic semiconductors (OS) have proven intriguing possibilities in the field of spintronics. Devices realized on the basis of the so-called spinterfaces [9,10], i.e., interfaces between a magnetic layer (ML) and an OS, show indeed enhanced spin lifetimes and conducting paths with respect to their inorganic counterparts.

It is known that the spin-transport process in such devices can be influenced by new electronic states arising at the interface, as a result of the hybridization between the d-band of the ML and the molecular orbitals of the OS [11]. On the other hand, the OS may itself influence the magnetism of the surface to which it is coupled [12,13] or induce a magnetic character into a surface that would be otherwise non-magnetic [**?**]. Accordingly, achieving information and control over the electronic and magnetic properties of the interface, as well as over the occurring chemical interactions, may enable to better tailor such systems - via a suitable choice of the materials involved - in view of practical applications.

In recent works [14-16] some of us focused on the C_{60}/Fe(001) interface, both on the experimental and theoretical viewpoint. We demonstrated that the induced magnetic properties on the molecules depend on the spin polarization of the substrate states interacting with the molecule itself and by their decay toward vacuum. In particular we showed that the insertion of a thin two-dimensional Cr_4O_5 film at the spinterface is able to enhance the spin-injection process, inducing a larger spin polarization of the C_{60} molecules with respect to the clean substrate case.

Here we analyse the system in a different perspective, i.e., focusing on the capability of the organic layer to modify the magnetic properties of the Cr_4O_5/Fe(001) surface. The Cr atoms in an isolated Cr_4O_5 layer would naturally arrange with antiferromagnetic (AFM) ordering. The interaction with the Fe substrate turns the AFM intra-layer ordering into a ferromagnetic (FM) one [15] leading to a magnetization direction of Cr atoms opposite to that of Fe ones (inter-layer AFM coupling).

The magnetic ordering at the surface is intimately related to the local symmetry of the electronic states involved in the magnetic interaction. It is reasonable to expect that, by controlling the local symmetry of the spinterface states –for example by tuning the local substrate-molecule interaction– the magnetic ordering of the Cr atoms in the oxide layer could be modified. We verified that the induced magnetic properties on the molecule are mildly dependent on the adsorption geometry. On the other hand we cannot assume that the same holds for the magnetic properties of the oxide substrate layer. Here we explore the possibility of inducing a rearrangement of the surface magnetic ordering by tailoring the C_{60} adsorption on Cr_4O_5/Fe(001), by means of calculations for a fully relaxed overlayer of C_{60} molecules in different high symmetry adsorption geometries.

We show that the adsorption of a C_{60} layer can indeed restore the AFM ordering in the underlying Cr_4O_5. Moreover, by moving the molecules onto different adsorption sites it is possible to switch the Cr_4O_5 ordering from AFM to FM, or to induce a nontrivial magnetic patterning involving the Cr atoms in the oxide layer. The possibility to control the adsorption geometry through experimental techniques is not a remote scenario: recent works demonstrate indeed that the local adsorption configuration of organic molecules can be controlled by means of a STM tip [17-19].

The total energy calculations performed in this work allow us to identify the most stable configurations that could lead to the desired magnetic pattern. The study of the possible adsorption configurations and the associated diffusion barriers can shed light also on the nucleation mechanism, as recently done for the clean Fe(100) surface, where the competitive adsorbate-substrate and adsorbate-adsorbate interactions give rise to a mixed layered growth [20].

Results and discussion

The system under examination offers several possible adsorption configurations, depending on the adsorption site and the relative orientation between the C_{60} and the surface. We explore here nine high symmetry cases, by combining three possible adsorption sites - namely a surface vacancy, a Cr atom and an O atom - with three possible orientations of the fullerenes, facing towards the surface with a hexagonal ring, a pentagonal one, and a C-C covalent bond, respectively.

Upon relaxation the system appears as reported in Figure 1. Major details regarding the surface structure can be found in our previous studies [21]. The configurations with adsorbed C_{60} reported in the two upper rows of Figure 1 (adsorption via a hexagon or a pentagon) show a partial roto-translation of the molecules on the surface, implying that the hexagon/pentagon is not perfectly centred on the chosen adsorption site. The leading force influencing the fullerene roto-translation seems to be the interaction with O atoms: indeed, with the exception of the adsorption on O, the molecules shift in order to get two C atoms facing to the surface close to two O atoms of the substrate. Differently, when C_{60} faces the surface with a C-C bond the starting adsorption site remains almost unaltered upon relaxation.

The energetically most stable configuration turns out to be the central one in Figure 1, where a vacancy acts as adsorption site and a pentagon faces to the surface (shortcut to *Pent/Vac* hereafter). We take this as a reference, and report in Table 1 the energy differences, ΔE_{ads}, of the other configurations. For what concerns the various configurations, we find no evident trend in the adsorption energy defining a preferential adsorption site or molecular orientation.

The equilibrium distance of the fullerenes from the surface, evaluated as the difference between the average $\hat{z}$ coordinate of the C atoms in the pentagon/hexagon/bond and of the Cr layer, ranges between 2.67 and 3.15 Å. It is worth noting that the O atoms lie 0.25 Å further out from the Cr plane [21], resulting in a smaller distance between the molecule and the O atom acting as adsorption site. This confirms the tendency of the molecule to interact with oxygen. The most stable configuration is characterized by the intermediate distance of 2.89 Å; in this case, the average distance between the C atoms of the pentagon and the O atoms nearest to the vacancy amounts to 2.67 Å.

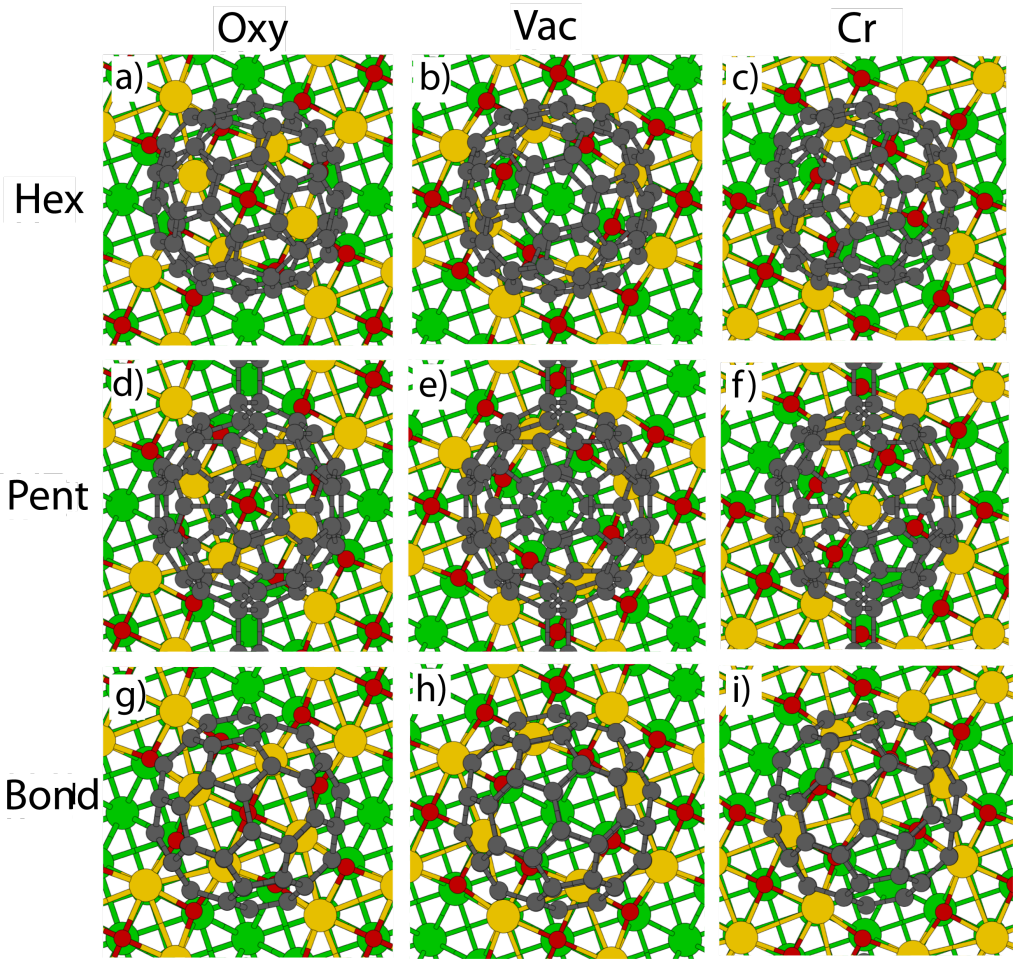

Figure 1: Top view of the explored configurations, depending on adsorption site and relative orientation between C_{60} and Cr_4O_5. The color code is as follows: Fe - green, Cr - yellow, O - red and C - grey.

In Table 1 we also report the charge transfer induced by the C_{60} adsorption, averaged for each atomic species. In all the explored configurations there is a partial electron transfer from the surface to the molecule, whose entity is obviously related to the adsorption distance. The depletion of charge on the O atoms is larger than in the Cr atoms while the contribution from the underlying Fe substrate is smaller.

The analysed configurations display different magnetic properties, in particular for what concerns the magnetic alignment of the surface Cr atoms, as can be observed in the spin densities reported in Figure 2. Here, we cut the three-dimensional spin distribution onto the plane passing through the Cr atoms in the Cr_4O_5; the position of Cr and O atoms, and the vacancies in the unit cell are

Table 1: Adsorption energy (with respect to the low energy configuration), distance and Löwdin partial charge for each atomic species. Charge differences Δq are evaluated with respect to the isolated systems Cr_4O_5/Fe(001) and C_{60}, both considered in their ground state. The adsorption distance d is given with respect to the Cr plane.

Configuration	ΔE_{ads} [eV]	d [Å]	Δq [10^{-2} e$^-$/atom]			
			Fe	Cr	O	C_{60}
Pent/Vac	0.00	2.89	-1.24	-1.83	-9.01	2.92
Pent/Oxy	0.26	2.74	-1.02	-5.96	-8.22	3.22
Hex/Oxy	0.41	2.67	-1.17	-6.38	-9.02	3.47
Bond/Cr	0.61	2.64	-1.28	-2.56	-8.99	3.02
Hex/Cr	0.72	3.15	-1.09	-3.31	-7.73	2.64
Hex/Vac	1.12	2.97	-1.25	-1.96	-9.17	2.94
Pent/Cr	1.59	3.06	-0.79	-5.18	-6.99	2.75
Bond/Vac	1.95	2.78	-1.12	-1.90	-8.83	2.83
Bond/Oxy	4.65	2.79	-1.17	-3.55	-8.44	3.05

indicated in the central panel of Figure 2. They can be identified also on the basis of their different spin density: very large and flower-shaped on Cr atoms, small on O atoms and zero (white) in correspondence of the vacancies.

We find that the adsorption of C_{60} in the most stable *Pent/Vac* configuration induces a recovery of the AFM ordering of the nearest neighbour Cr atoms (central panel in Figure 2), which would be the preferred magnetic state in absence of the underlying Fe substrate. Indeed some of us have already shown [14] that the interaction between the Cr_4O_5 overlayer and the Fe substrate destabilizes the AFM coupling in the oxide layer, leading to a intra-layer FM alignment of the Cr atoms, that are in turn AFM coupled to the Fe substrate.

The same AFM pattern, typical of the isolated oxide layer, occurs for the other two configurations featuring a vacancy as adsorption site (*Hex/Vac* and *Bond/Vac*, ordered by increasing energy). In three configurations (*Pent/Oxy*, *Hex/Oxy* and *Pent/Cr*) the final pattern is instead FM, i.e., with the magnetic moment of all the Cr atoms parallel to each other. For the remaining cases (*Hex/Cr*, *Bond/Oxy* and *Bond/Cr*), a different magnetic patterning appears on the surface, characterized by the spinflip of certain Cr atoms only.

We report in Table 2 the magnetic moments calculated for the different species. In particular we report the average values for the outermost Fe substrate layer, for the Cr and O atoms in the oxide

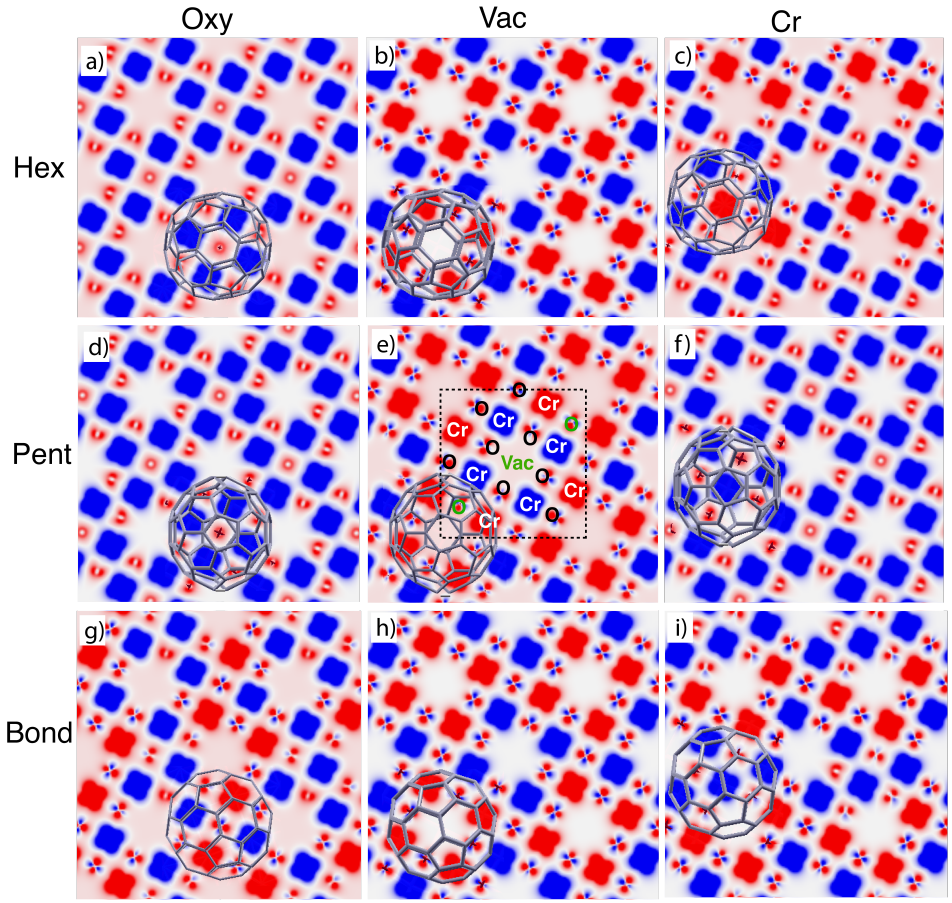

Figure 2: Spin polarization $\rho_{up} - \rho_{down}$ for each pattern (top view). A cut on the surface plane passing through the Cr atoms is reported with an isosurface value of 0.02 Å^{-3}. Red and blue area corresponds to positive and negative value of spin polarization, respectively.

layer, for the whole C_{60} molecule and for the C atoms facing to the surface. In the non-FM cases, we give the average values separately for the positively and negatively polarized Cr atoms. The average magnetization of the Fe surface layer is about 2.6 μ_B showing a reduction with respect to the clean surface value (3.0 μ_B).

Notably, the net magnetization of the Cr atoms in the oxide layer is always opposite to the underlying Fe one, as in absence of molecules, confirming the antiferromagnetic coupling between the overlayer and the substrate evidenced by the experiments [14]. Indeed, also in the configurations

Table 2: Average magnetic moment for outermost Fe atoms, Cr atoms, C_{60} molecule and C atoms closest to the surface, belonging to a hexagon, a pentagon or a bond. When two values are present, those indicate the average magnetic moment for atoms with positive (aligned to Fe one) and negative spin polarization.

Config.	μ [μ_B/atom]		μ [10^{-2} μ_B/atom]		
	Fe	Cr	O	C_{60}	$C_{Hex/Bond/Pent}$
Pent/Vac	2.25	-0.31 (2.26 / -2.88)	1.5	0.1	0.5
Pent/Oxy	2.32	-2.96	2.6	-0.6	-0.9
Hex/Oxy	2.32	-2.93	2.3	-0.4	-1.6
Bond/Cr	2.29	-0.87 (2.40 / -2.84)	1.8	-0.1	-0.2
Hex/Cr	2.32	-1.58 (2.45 / -2.92)	2.4	-0.1	-6.7
Hex/Vac	2.25	-0.31 (2.25 / -2.88)	1.5	0.2	1.1
Pent/Cr	2.32	-3.00	2.7	-0.4	-1.4
Bond/Vac	2.24	-0.29 (2.30 / -2.88)	1.4	0.1	0.6
Bond/Oxy	2.30	-1.55 (2.46 / -2.89)	3.4	-0.1	-0.3

with intra-layer AFM ordering the magnetic moment of opposite Cr atoms is not identical, and the total magnetization does not cancel out.

The magnetic moment of the C atoms is three orders of magnitude smaller than that of the Cr atoms and its sign depends on the adsorption configuration. The largest magnetic moments on the molecule are found for the FM configurations and have the same sign of the magnetic moment of the Cr atoms. On the contrary, for the equilibrium configuration, and the other cases with AFM ordering of the Cr atoms, the net magnetic moment on the molecule and on C atoms facing to the surface is opposite to that of the Cr_4O_5 layer, but has the same sign as that of the Cr atoms closest to the molecule (see Figure 2).

In the FM systems the magnetic moment of single O atoms is opposite to that of the surrounding Cr atoms, resulting into a net positive magnetization. In the AFM ones the magnetization of O atoms nearby the spin-flipped Cr atoms is reduced, leading to a smaller positive net magnetic moment. It is worth noting that the configurations that display AFM ordered Cr atoms also display a peculiar symmetry of the spin density on the O atoms which resemble the in-plane p-orbitals (see Figure 2). Differently, in the FM cases such feature is absent and the spin density on the O atoms shows an s-like symmetry. This peculiarity can be observed also in the freestanding Cr_4O_5 over-

layer by switching the system from the AFM ground state to the high-energy FM configuration (not shown).

This evidence suggests that the AFM coupling between the Cr atoms may be mediated by the O orbitals that tailor also the interaction with the molecule.

In order to give a deep insight into the induced magnetic properties at the interface, we consider the Projected Density of States (PDOS) of the different atomic species that, together with a detailed analysis of the spin- and orbital- dependent Mülliken populations, can help in understanding the driving mechanism for spin-flip of the Cr atoms.

In Figure 3 we report the PDOS for the two lowest-energy configurations, namely *Pent/Vac* and *Pent/Oxy*, that exhibit a different magnetic ordering of the Cr atoms in the oxide layer. We consider the average d component of Fe surface layer and of the Cr atoms and the average p component of O atoms in the oxide layer and of C atoms facing to the surface.

The Fe PDOS is similar in the two configurations, demonstrating that the underlying substrate is on average weakly affected by the different adsorption conditions. The spin polarization of the Cr atoms in the *Pent/Oxy* configuration is opposite to that of the Fe surface layer, as already evidenced in our past study. Differently, in the AFM configuration induced by C_{60} adsorption one half of the Cr atoms are spin-flipped, with magnetization oriented parallel to the substrate (Cr_{up}) while the other remain antiferromagnetically coupled to the substrate (Cr_{down}). The asymmetry between filled states of Cr_{up} and Cr_{down} atoms gives rise to the net negative magnetic moment reported in Table 2.

For what concerns the O atoms, they display a negligible spin polarization at the Fermi level in the *Pent/Oxy* configuration, which is enhanced in the *Pent/Vac* case due to the presence of majority spin states. From the analysis of the m-resolved PDOS, reported in Figure 4, we can assign these states mainly to p_z orbitals, that are emptied due to the charge transfer toward the molecule. The majority spin O p_z component (red line) in the *Pent/Oxy* configuration displays indeed an occupied feature at -0.8 eV which is shifted beyond the Fermi level in the *Pent/Vac* case. The p_z charge donated by O atoms to the C atoms in the pentagon is the major source of charge transfer to the

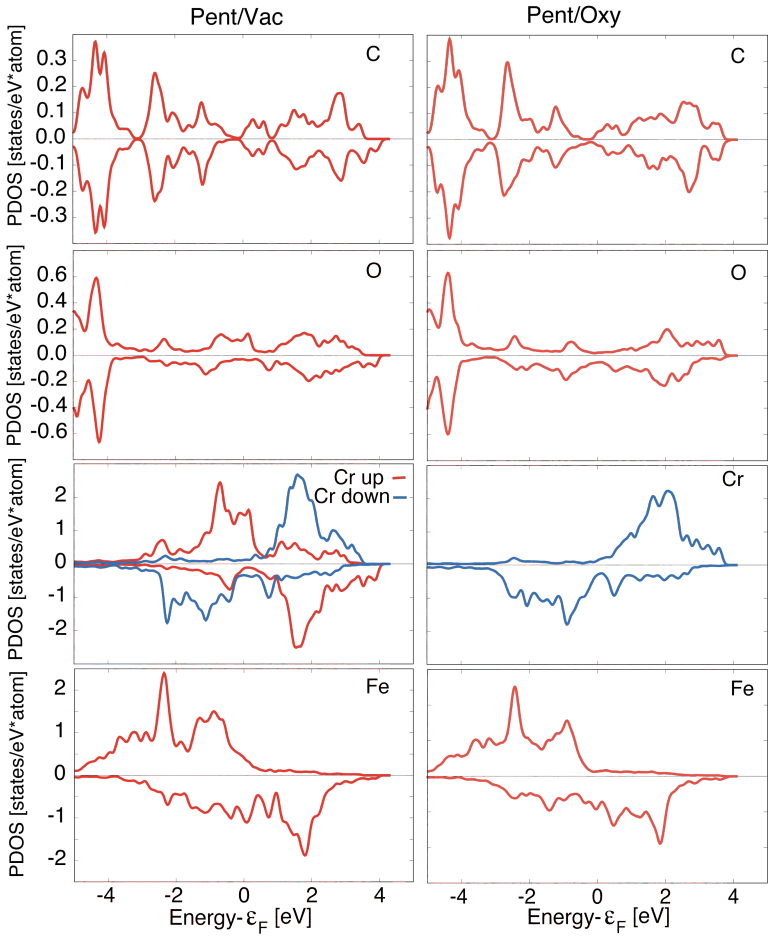

Figure 3: PDOS on Fe and Cr (d component), O and C atoms facing to the surface (p-component) for the *Pent/Vac* (left) and *Pent/Oxy* (right) configurations. Two representative Cr atoms with opposite polarization are reported for the AFM configuration.

molecules in the *Pent/Vac* configuration, bypassing the Cr contribution (see Table 1). Indeed in this configuration the spatial proximity between O atoms and the C atoms in the pentagon facilitates the interaction between the two species.

Also the in-plane majority spin p-states of O atoms display a small increase of the spectral weight at the Fermi level with respect to the *Pent/Oxy* case, due to the charge transfer to the nearby Cr atoms. The majority spin character of the charge donated by O atoms explains the reduction of the magnetic moment of O in the AFM configurations with respect to the FM one. Accordingly, the magnetic moment of the molecule is positive. Being the in-plane charge transfer strongly directional, the spin-density displays the asymmetry observed in Figure 2 with negative lobes pointing

toward the Cr atoms. As a consequence the nearest neighbour Cr atoms undergo a spin-flip to stabilize the magnetic interaction, as in the free-standing overlayer.

Differently, in the *Pent/Oxy* configuration the charge trasferred to the molecule comes from the Cr atoms due to their spatial proximity with the pentagon facing to the surface. The charge donated to the molecule has negative spin character, being transferred from the spin-down d states of Cr to the s states of the molecule. Some electronic charge is also donated by the O atoms, with the same amount for both spin up and down, leading to a net negative magnetic moment of the molecule, while that of O atoms is unaltered with respect to the Cr_4O_5/Fe(001).

On the basis of these results we can infer that the AFM patterning of the Cr atoms in the oxide layer is stabilized by the interaction between O atoms and the molecule, that induces a spin asymmetry in the Cr_4O_5 plane able to decouple some Cr atoms from the substrate and to destroy the substrate-induced FM ordering between Cr atoms.

To conclude our analysis, we report some energetic considerations relative to the magnetic switching between the AFM and FM ordering in the Cr_4O_5 layer.

Once the C_{60} molecules are adsorbed in the most stable *Pent/Vac* configuration, the transition to *Pent/Oxy* and thus to FM ordering can be obtained with an energetic cost of 0.26 eV. Compared to the energetic cost for the FM/AFM switching of the clean Cr_4O_5/Fe(001) surface (note that in this case the ground state is FM), amounting to 1.12 eV in the $(\sqrt{10} \times \sqrt{10})R{-}18.4^\circ$ cell, this mechanism results energetically more convenient as well as easier to be realized.

It is worth noting that the energetic cost reported above includes two contributions: the structural one, related to the shift onto a different adsorption site, and the magnetic cost associated to the spin-flip of certain Cr atoms. The difference in energy from the *Pent/Oxy* to the *Pent/Vac* adsorption site, evaluated keeping the FM ordering of the Cr atoms fixed, amounts to +0.04 eV, corresponding to a temperature of 464 K, i.e. in the range of typical temperatures reached with annealing.

On the other hand, the energy gain upon allowing the system in the *Pent/Vac* free to relax in the AFM ground state is −0.30 eV (the sum of these contributions gives indeed the value $\Delta E_{ads} = 0.26$

eV, as reported in Table 1). The quite large absolute value of the magnetic contribution compared to the structural one demonstrates that the AFM ordering realized in the *Pent/Vac* configuration is stabilized by magnetic effects more than structural ones.

Furthermore, by comparing the absolute value of the FM/AFM energy difference with and without the molecule (0.30 eV versus 1.12 eV) it is evident that the presence of the molecule reduces the magnetic coupling between the Cr_4O_5 and the Fe substrate which is responsible of the forced magnetic ordering in the overlayer. Indeed, in the absence of the substrate the energy cost for the AFM/FM switching in the Cr_4O_5 layer would be extremely small (0.04 eV).

Conclusions

In conclusion, in the present work we demonstrated that the adsorption of a C_{60} layer on the Cr_4O_5/Fe(001) surface can tailor the intralayer magnetic ordering between the Cr atoms restoring the AFM configuration proper of the freestanding oxide overlayer, destroyed by the interaction with the substrate. Moreover the AFM/FM switching is possible via a precise control on the adsorption site of the molecule that could be achieved by exploiting the ad hoc positioning via the STM tip or modified by thermal annealing. The presence of an organic layer at the interface - be it C_{60} or something else - is expected to be a notable step further towards the realization of more efficient spintronic devices; furthermore, attaining a patterning on the surface by means of the adsorption of organic species is expected to be far easier than creating it *ad hoc* on the bare Cr_4O_5/Fe(001) by exploiting magnetic or electric means. Therefore, our results may be considered as a route towards the design of desired magnetic patterning by means of adsorbed organic molecules.

Computational methods

Ab initio calculation have been performed in the framework of Density Functional Theory (DFT), following the scheme of our previous works [14-16].

We have used a plane-wave ultrasoft pseudopotential method [22], as implemented in the PWSCF code of the Quantum ESPRESSO distribution [23,24]. We treat the DFT exchange-correlation term

by using the vdW-DF-c09x functional [25,26], also including van der Waals interaction between the C_{60}s and the underlying surface.

The clean Cr_4O_5/Fe(001) substrate exhibits an experimentally-observed $(\sqrt{5} \times \sqrt{5})R26.6^\circ$ reconstruction [21], featuring a regular array of Cr vacancies. For the calculations, the introduction of a C_{60} overlayer calls for the employment of a larger periodically repeated cell: we employ a $(\sqrt{10} \times \sqrt{10})R{-}18.4^\circ$ supercell, whose area is twice that of the clean surface. The Cr_4O_5 layer is supported by a four-layers Fe slab, separated from its replicas along the $\hat{z}$ direction by a 25 Å-thick vacuum layer.

Equilibrium geometries were obtained by letting the C atoms of the fullerene molecules free to relax, up to the desired convergence threshold for the forces (0.001 Ry/Bohr).

A Monkhorst-Pack grid [27] was adopted for the surface Brillouin zone sampling, equivalent to a 14×14 mesh in the surface unit cell of Fe(001); the kinetic energy cutoffs were set to 55 Ry for the plane-wave expansion and 280 Ry for the effective potential and charge density.

To disentangle magnetic contributions to energy differences, we have performed additional self-consistent calculations constraining the magnetic moment at specific atoms and keeping the geometry unchanged.

Acknowledgements

We acknowledge the CINECA award under the ISCRA initiative (grants IscrC-SPINOF2-HP10C3S9Z0 and IscrC-APOCAPOF-HP10CB0ZW2), for the availability of high performance computing resources and support.

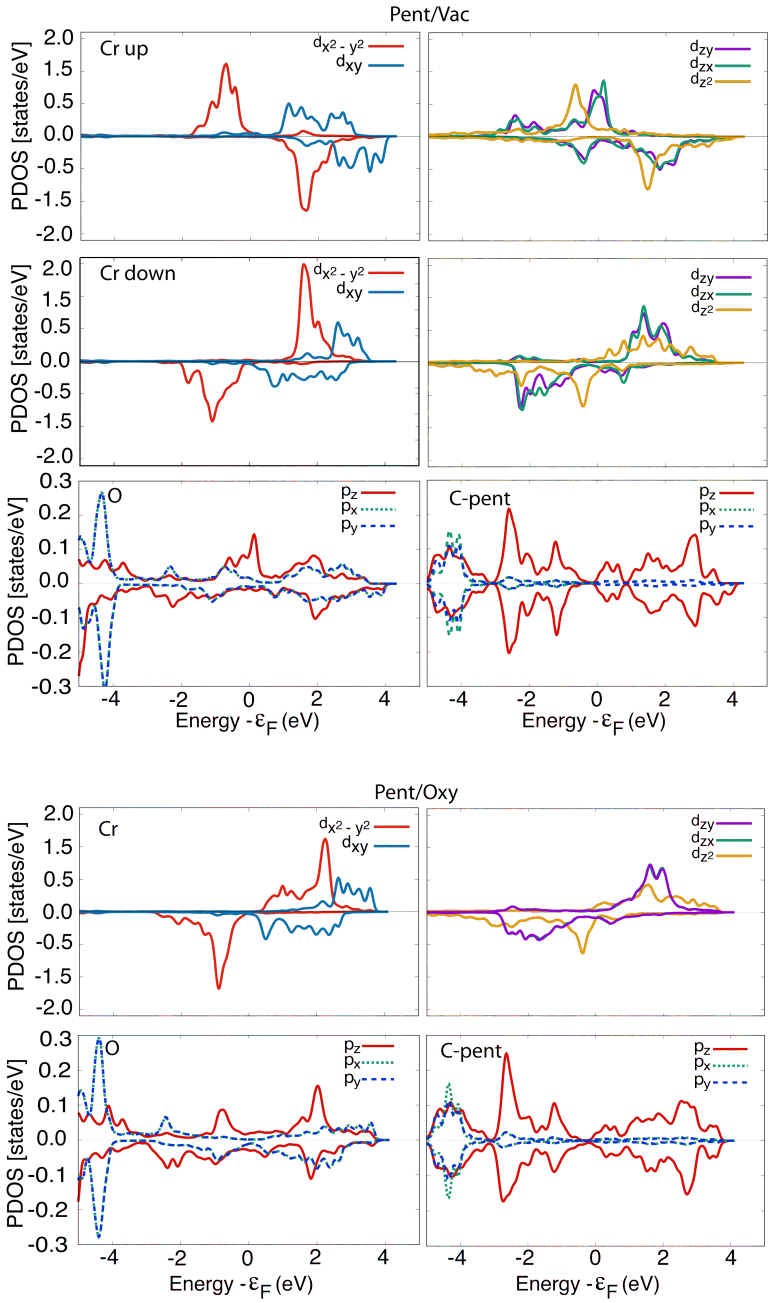

Figure 4: *d* component of the PDOS of Cr atoms resolved in *m* components for the *Pent/Vac* and *Pent/Oxy* configurations.

References

1. Brovko, O. O.; Ruiz-Díaz, P.; Dasa, T. R.; Stepanyuk, V. S. *J. Phys.: Condens. Matter* **2014**, *26*, 093001.

2. Myers, E. B.; Ralph, D. C.; Katine, J. A.; Louie, R. N.; Buhrman, R. A. *Science* **1999**, *285*, 867.

3. Carmeli, I. *J. Chem. Phys.* **2003**, *118*, 10372.

4. Callsen, C. V. K. N. A. N. . B. S., M. *Phys. Rev. Lett.* **2013**, *111*, 106805.

5. Hernando, A.; Crespo, P.; García, M. A. *Phys. Rev. Lett.* **2006**, *96*, 57206.

6. Achilli, S.; Caravati, S.; Trioni, M. I. *J. Phys. Condens. Matter* **2007**, *19*, 305021.

7. Del Castillo, E.; Cargnoni, F.; Achilli, S.; Tantardini, G.; Trioni, M. *Surf. Sci.* **2015**, *634*, 62.

8. Ben Dor, O.; Yochelis, S.; Radko, A.; Vankayala, K.; Capua, E.; Capua, A.; Yang, S.; Baczewski, L. T.; Papworth Parkin, S. S.; Naaman, R.; Paltiel, Y. *Nat. Commun.* **2017**, *8*, 14567.

9. Sanvito, S. Nat. Phys. **2010**, *6*, 562.

10. Cinchetti, M.; Dediu, V. A.; Hueso, L. E. *Nat. Materials.* **2017**, *16*, 507.

11. Delprat, S.; Galbiati, M.; Tatay, S.; Quinard, C., B. anf Barraud; Petroff, F. *J. Phys. D: Appl. Phys.* **2019**, *51*, 473001.

12. Bairagi, K.; Bellec, A.; Repain, V.; Chacon, C.; Girard, Y.; Garreau, Y.; Lagoute, J.; Rousset, S.; Breitwieser, R.; Hu, Y.-C.; Chao, Y. C.; Pai, W. W.; Li, D.; Smogunov, A.; Barreteau, C. *Phys. Rev. Lett.* **2015**, *114*, 247203.

13. Denk, M.; Queteschiner, D.; Hohage, M.; Navarro-Quezada, A.; Zeppenfeld, P. *J. Appl. Phys.* **2019**, *125*, 142902.

14. Brambilla, A.; Picone, A.; Giannotti, D.; Calloni, A.; Berti, G.; Bussetti, G.; Achilli, S.; Fratesi, G.; Trioni, M. I.; Vinai, G.; Torelli, P.; Panaccione, G.; Duò, L.; Finazzi, M.; Ciccacci, F. Nano Lett. **2017**, *17*, 7440.

15. Calloni, A.; Fratesi, G.; Achilli, S.; Berti, G.; Bussetti, G.; Picone, A.; Brambilla, A.; Folegati, P.; Ciccacci, F.; Duò, L. Phys. Rev. B **2017**, *96*, 085427.

16. Brambilla, A.; Picone, A.; Achilli, S.; Fratesi, G.; Lodesani, A.; Calloni, A.; Bussetti, G.; Zani, M.; Finazzi, M.; Duò, L.; Ciccacci, F. *J. App. Phys.* **2019**, *125*, 142907.

17. Liu, L.; Liu, S.; Chen, X.; Li, C.; Ling, J.; Liu, X.; Cai, Y.; Wang, L. *Sci. Rep.* **2013**, *3*, 3062.

18. Liu, J.; Li, C.; Liu, X.; Lu, Y.; Xiang, F.; Qiao, X.; Cai, Y.; Wang, Z.; Liu, S.; Wang, L. *ACS Nano* **2014**, *8* (12), 12734.

19. Wei, S.; Wang, Z.; Jin, J.; Xu, H.; Lu, Y.; Wang, L. *Nanotechnology* **2018**, *29*, 395301.

20. Hu, L.; Pang, R.; Gong, P.; Shi, X. J.Phys. Chem. C **2019**, *123*, 15477.

21. Picone, A.; Fratesi, G.; Riva, M.; Bussetti, G.; Calloni, A.; Brambilla, A.; Trioni, M. I.; Duò, L.; Ciccacci, F.; Finazzi, M. Phys. Rev. B **2013**, *87*, 085403.

22. Vanderbilt, D. Phys. Rev. B **1990**, *41*, 7892.

23. Giannozzi, P.; Baroni, S.; Bonini, N.; Calandra, M.; Car, R.; Cavazzoni, C.; Ceresoli, D.; Chiarotti, G. L.; Cococcioni, M.; Dabo, I.; Dal Corso, A.; de Gironcoli, S.; Fabris, S.; Fratesi, G.; Gebauer, R.; Gerstmann, U.; Gougoussis, C.; Kokalj, A.; Lazzeri, M.; Martin-Samos, L.; Marzari, N.; Mauri, F.; Mazzarello, R.; Paolini, S.; Pasquarello, A.; Paulatto, L.; Sbraccia, C.; Scandolo, S.; Sclauzero, G.; Seitsonen, A. P.; Smogunov, A.; Umari, P.; Wentzcovitch, R. M. Journal of Physics: Condensed Matter **2009**, *21*, 395502.

24. Giannozzi, P.; Andreussi, O.; Brumme, T.; Bunau, O.; Nardelli, M. B.; Calandra, M.; Car, R.; Cavazzoni, C.; Ceresoli, D.; Cococcioni, M.; Colonna, N.; Carnimeo, I.; Corso, A. D.;

de Gironcoli, S.; Delugas, P.; Jr, R. A. D.; Ferretti, A.; Floris, A.; Fratesi, G.; Fugallo, G.; Gebauer, R.; Gerstmann, U.; Giustino, F.; Gorni, T.; Jia, J.; Kawamura, M.; Ko, H.-Y.; Kokalj, A.; Küçükbenli, E.; Lazzeri, M.; Marsili, M.; Marzari, N.; Mauri, F.; Nguyen, N. L.; Nguyen, H.-V.; de-la Roza, A. O.; Paulatto, L.; Poncé, S.; Rocca, D.; Sabatini, R.; Santra, B.; Schlipf, M.; Seitsonen, A. P.; Smogunov, A.; Timrov, I.; Thonhauser, T.; Umari, P.; Vast, N.; Wu, X.; Baroni, S. *Journal of Physics: Condensed Matter* **2017**, *29* (46), 465901.

25. Lee, K.; Murray, E. D.; Kong, L.; Lundqvist, B. I.; Langreth, D. C. Phys. Rev. B **2010**, *82*, 081101.

26. Cooper, V. Phys. Rev. B **2010**, *81*, 161104.

27. Monkhorst, H. J.; Pack, J. D. Phys. Rev. B. **1976**, *13*, 5188.